academicJournals

Vol. 8(12), pp. 451-458, 30 March, 2013
DOI: 10.5897/IJPS12.483
ISSN 1992-1950 © 2013 Academic Journals
http://www.academicjournals.org/IJPS

International Journal of Physical Sciences

Full Length Research Paper

Methodological approach of selecting a vibration indicator in monitoring bearings

O. Djebili[1]*, F. Bolaers[1], A. Laggoun[2] and J. P. Dron[1]

[1]Laboratoire Grespi/MAN UFR, Sciences Exactes and Naturelles Moulin de la Housse, BP 1039 51687 REIMS CEDEX 2, France.
[2]Department de physique, Faculté des Sciences UMBB Boumerdes, Algéria.

Accepted 5 March, 2013

A rolling bearing is an important element in a rotating machine. Whatever the operating conditions, it is subject to fatigue which causes spalling. In aiming to obtain the most possible real fatigue curve, the vibration level is shown according to different statistical indicators such as the RMS (Root Mean Square), the kurtosis, the crest value, the crest factor and the peak ratio, then to choose the best of them that is able to show the evolution of the bearing degradation. In this work, through the experimental vibratory follow up of the thrust bearing spall using different statistical indicators, we present an optimization methodology in order to find a most significant indicator that is able to characterize the damage evolution.

Key words: Bearing, vibration, analysis, vibration indicator, spalling.

INTRODUCTION

Bearings are among the most precise components in mechanical assemblies and are manufactured to very tight tolerances. They are normally found in most rotational equipment. The condition and health of bearing play an important role in the functionality and performance of these equipments. The main defect that may know a rolling bearing during normal operation is spalling. Really, this defect begins with subsurface cracks initiating within the raceway materiel. During the last state of service life, cracks might initiate and propagate and eventually reach the surface of the race dislodging a piece of metal from the surface. This results in what is known as spall. The vibration analysis is one of the most used methods to follow a spalling bearing of a rotating machine (Nagi and Mark, 2004). To establish the law of the bearing damage, it uses an efficient and appropriate vibration indicator. The purpose of this work focuses on the choice of the vibration indicator based on criteria that reflect greater significance of a default vibration signal. This generates a curve representative of damage.

Most of the research in this field has been done mainly about fatigue failure progression in ball bearings (Michael et al., 2001; Youngsik and Richard, 2007), diagnostics and residual live prediction of bearings (Nagi and Mark, 2004; Tallian, 1992) but most work only identifies the presence of defect, or at best differentiate based on qualitative measures such as light, medium or heavy damage (Hoeprich, 1992).

In this research, we will try to give an approach for improving the vibration measurement by choosing a vibration indicator to better characterize the evolution of the spalling in the bearing. We chose to study bearings with artificial defects. It was too long to tire bearings in normal use. We therefore simulated a spalling defect of

*Corresponding author. E-mail: omar_djebili@yahoo.com.

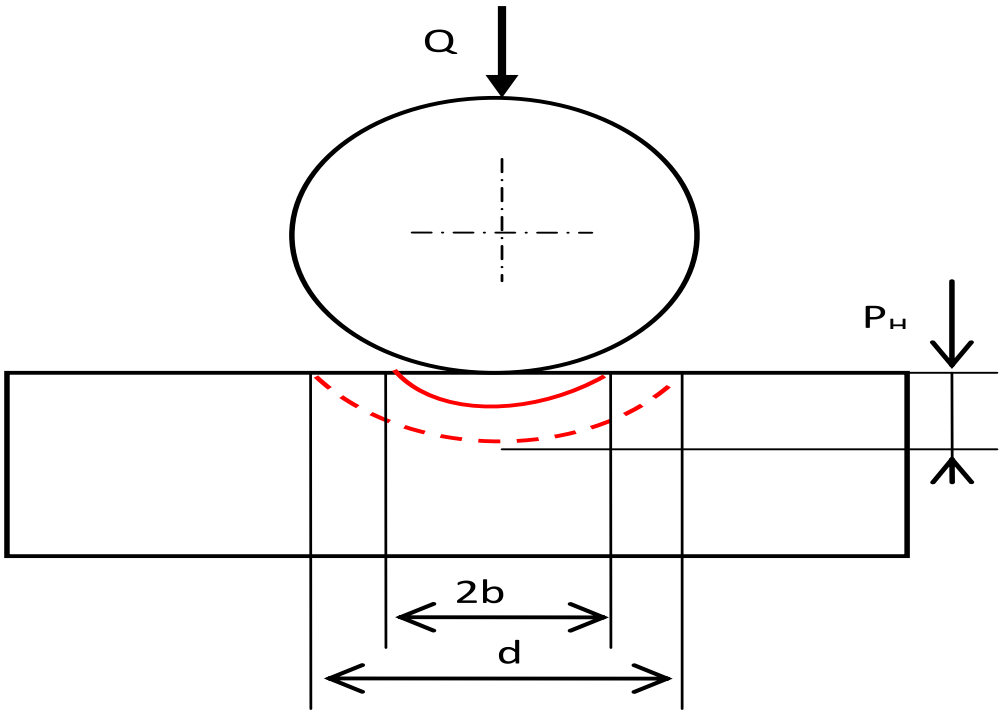

Figure 1. Contact sphere plan.

varying sizes on a series of thrust bearing. These artificial defects are created on the raceway of the thrust bearing ring by electro erosion.

PREPARATION OF EXPERIENCE AND SIMULATION OF FAILURE

We have chosen a thrust bearing type: FAG 51207 CZECH / ATK which has the following characteristics:

(i) Inner diameter Di_1 = 35 mm,
(ii) Inner diameter D_{i2} = 37 mm,
(iii) Outer diameter D = 62 mm,
(iv) Number of balls N_b = 12.

Before running spalling imprints on the thrust bearing ring, we need to do a calculation for determining the tool dimensions to use in the electro erosion machine. We consider the contact sphere-plan. Knowing the axial load (Q) applied on the bearing and the diameter of the ball (D_b), we determined:

(i) The semi-axis of the contact surface (Michel and René, 2005).

$$b = \sqrt[3]{\frac{3\pi(k_1 + k_2)N}{2(C_1 + C_1^{'} + C_2 + C_2^{'})}} \quad (1)$$

$$C_1 = \frac{1}{R_1}; C_1^{'} = \frac{1}{R_1^{'}}; C_2 = \frac{1}{R_2}; C_2^{'} = \frac{1}{R_2^{'}}$$

C_1 and C_2: maximum curvatures, $C_1^{'}$ and $C_2^{'}$: minimum curvatures, R_1 and $R_1^{'}$: ball radius, R_2 and $R_2^{'}$: track radius of a thrust bearing ring, k_1 and k_2: stiffness of the material.

$$k_1 = k_2 = \frac{1-\nu^2}{\pi E}$$

in our case, v = 0.3 : Poisson ratio, E = 210000 N/mm^2: elasticity module of the material, N = Q/12 : load on the ball (Figure 1).

(ii) Depth of Hertz (Michel and René, 2005; Daniel et al., 2002).

$$P_H = 0.5b \quad (2)$$

(iii) Radius of the ball bearing:

$$R = \frac{P_{rH}^2 + \left(\frac{d}{2}\right)^2}{2P_{rH}} \quad (3)$$

Imprint diameter

After a calculation of experience, we create spalling imprints by sinking using the electro erosion machine. The imprints are obtained according to tools (as ball) of different diameters previously calculated are shown in Figure 2. The hertz depth of the

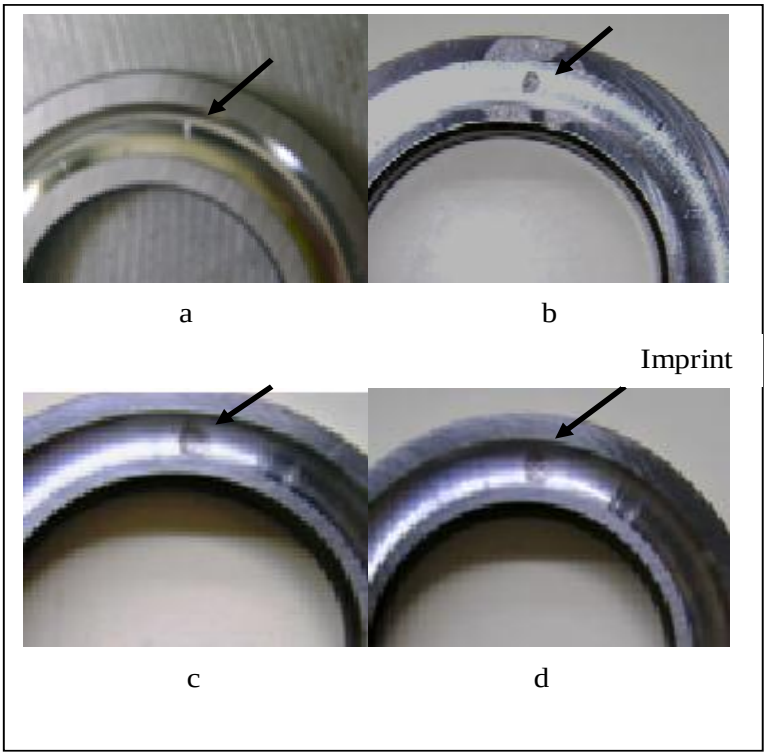

Figure 2. Spalling imprint on a thrust bearing ring (a) imprint Ø2.9; (b) imprint Ø3,9; (c) imprint Ø5,5; (d) imprint Ø6.4.

Table 1. Imprint depth.

Number of bearings	Ball diameter (mm)	Imprint depth (µm)
1	2.9	210
2	3.9	218
3	5.5	228
4	6.4	226

imprints obtained during the experience on four thrust bearings used is given in Table 1.

SPALLING VIBRATION MONITORING OF THE THRUST BEARING RING

The test bench consists of an electric motor, a cooling system, a mandrel to accommodate the thrust bearing and another to transmit the axial load from a hydraulic cylinder (Figure 3).

Vibratory statements of the thrust bearing

We note, at the trial bench, the vibration signals of simulated imprints (Youngsik and Richard, 2007) corresponding to different operating conditions (speed, load and frequency range). The tests are performed for various rotating speeds (600, 1200 and 1800 rpm), with two axial loads (2000 and 3000 daN). Measurements were taken at different frequencies range (1, 5 and 20 kHz).

Signals analysis

Vibration analysis starts with a time-varying, real-world signal from a transducer or sensor. From the input of this signal to a vibration measurement instrument, a variety of options are possible to analyze the signal. Let us take a look at the block diagram for a typical signal path in an instrument, as shown in Figure 4.

Vibration recordings were obtained on a test bench through a chain of acquisition as time signals. These time signals are then processed according to the diagram in Figure 4. To measure a spalling, we used statistical indicators that can be calculated through various stages of signal processing of Figures 5 and 6.

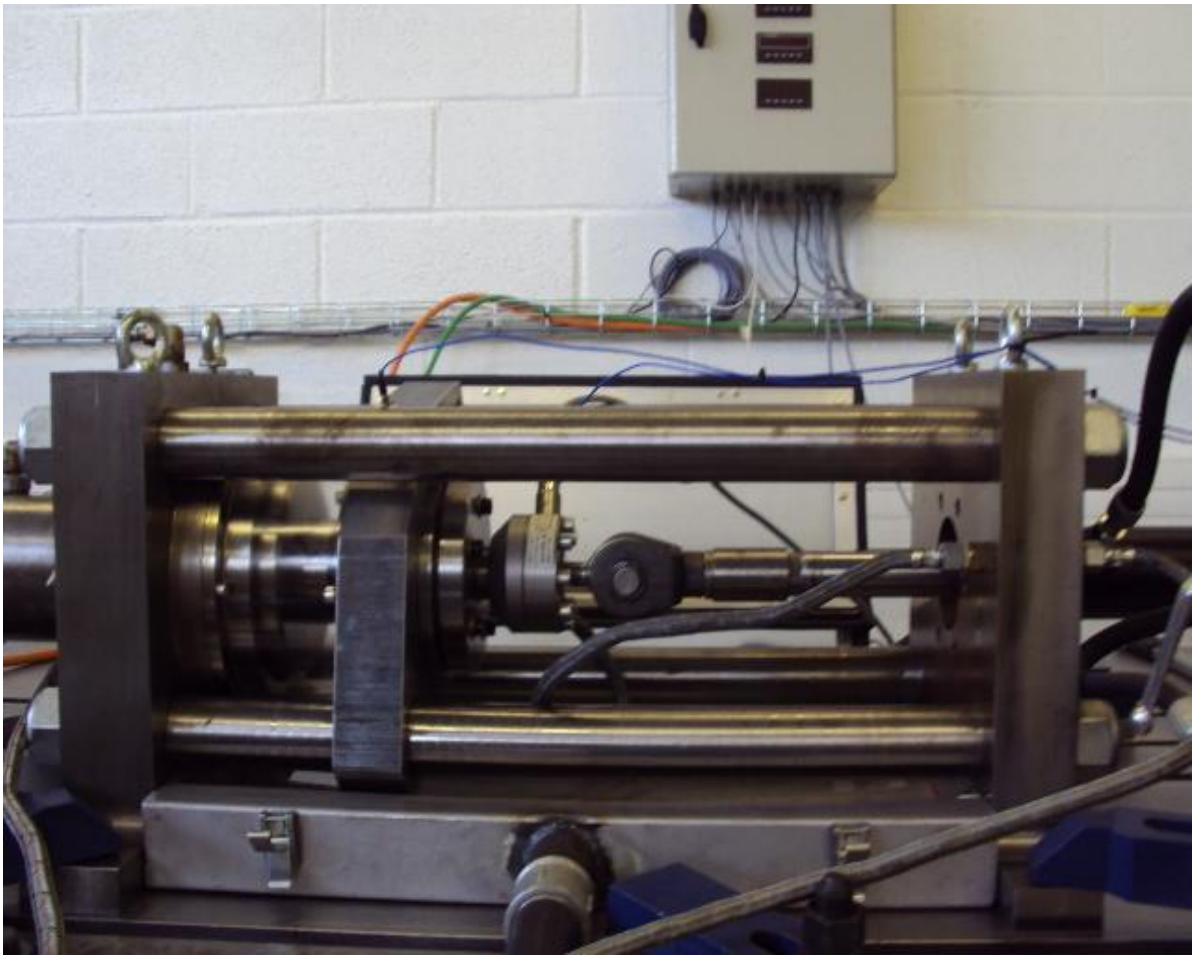

Figure 3. Image of the bearing test bench.

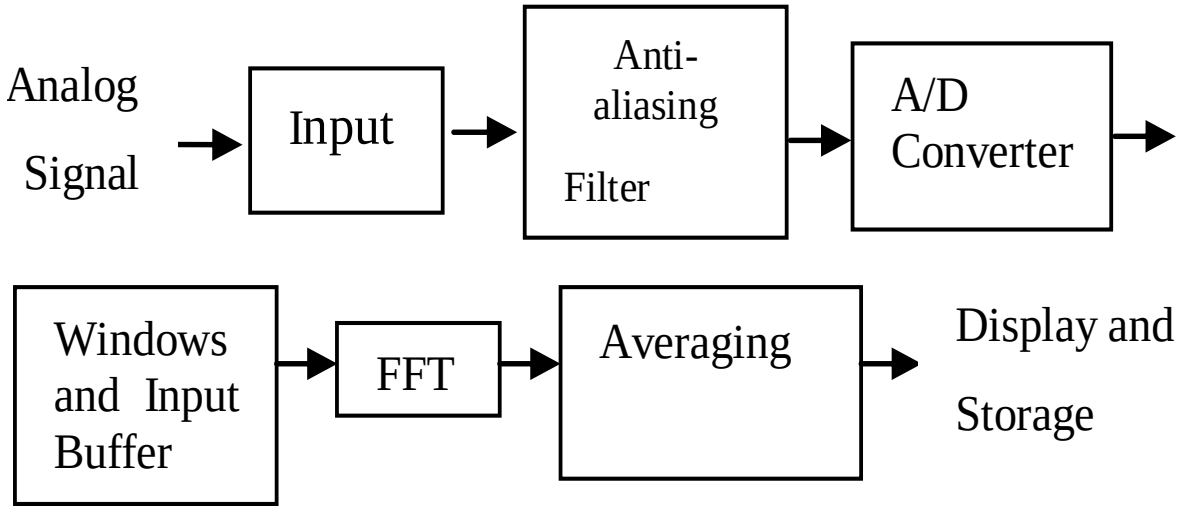

Figure 4. Typical signal path.

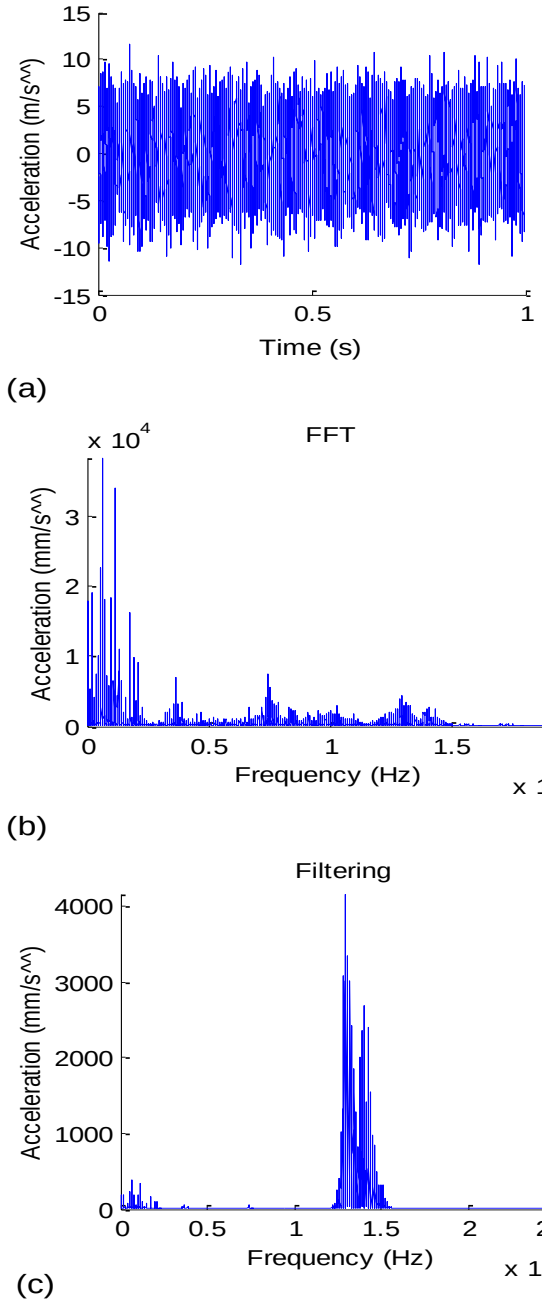

Figure 5. Signals analysis of undamaged bearing: (a) time domain signal, (b) frequency domain signal, (c) signal filtered at frequency band [13-15 kHz].

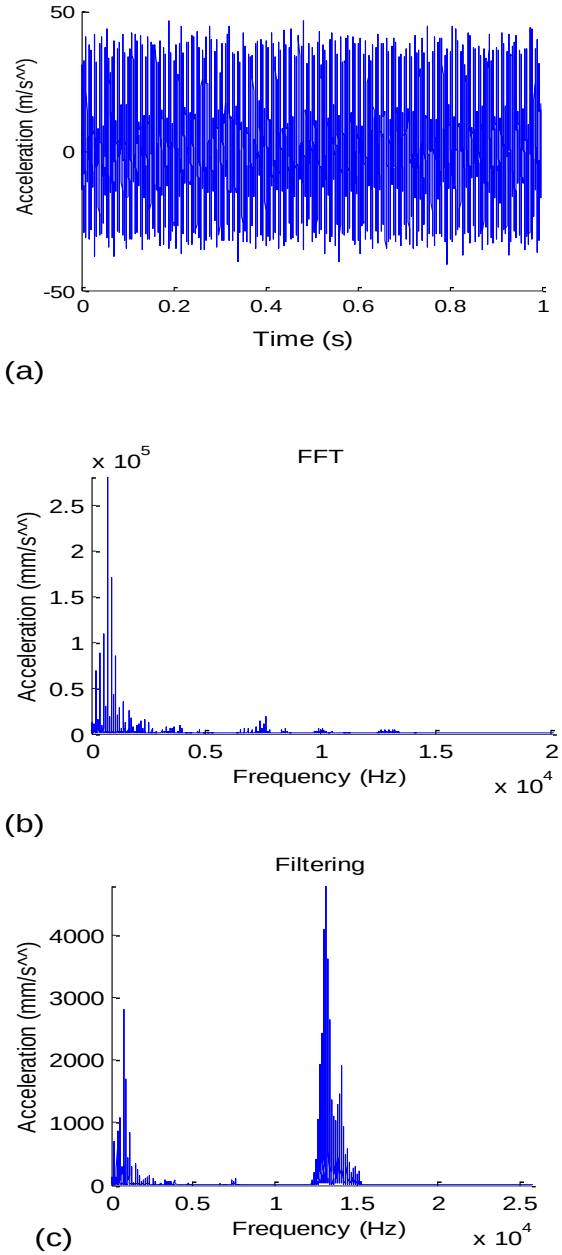

Figure 6. Signals analysis of failure detection: (a) time domain signal, (b) frequency domain signal, (c) signal filtered at frequency band [13-15 kHz].

Figure 6a shows a vibration signal at the time domain of damage which is the first to get but it is insufficient to quantify the severity of the defect. The time domain signal is converted to a vibration spectrum, which shows the signal in the frequency domain (Figure 6b). The conversion from time domain to frequency domain is done with a fast Fourier transformation (FFT). Then the vibration spectrum is filtered (Figure 6c) to make it more clear and precise. The spalling of the thrust bearing appears with a filtering in a high frequency band (Robert and Jerome, 2011).

Study of the spalling evolution

(1) Using classical vibratory indicators: We use a Matlab program

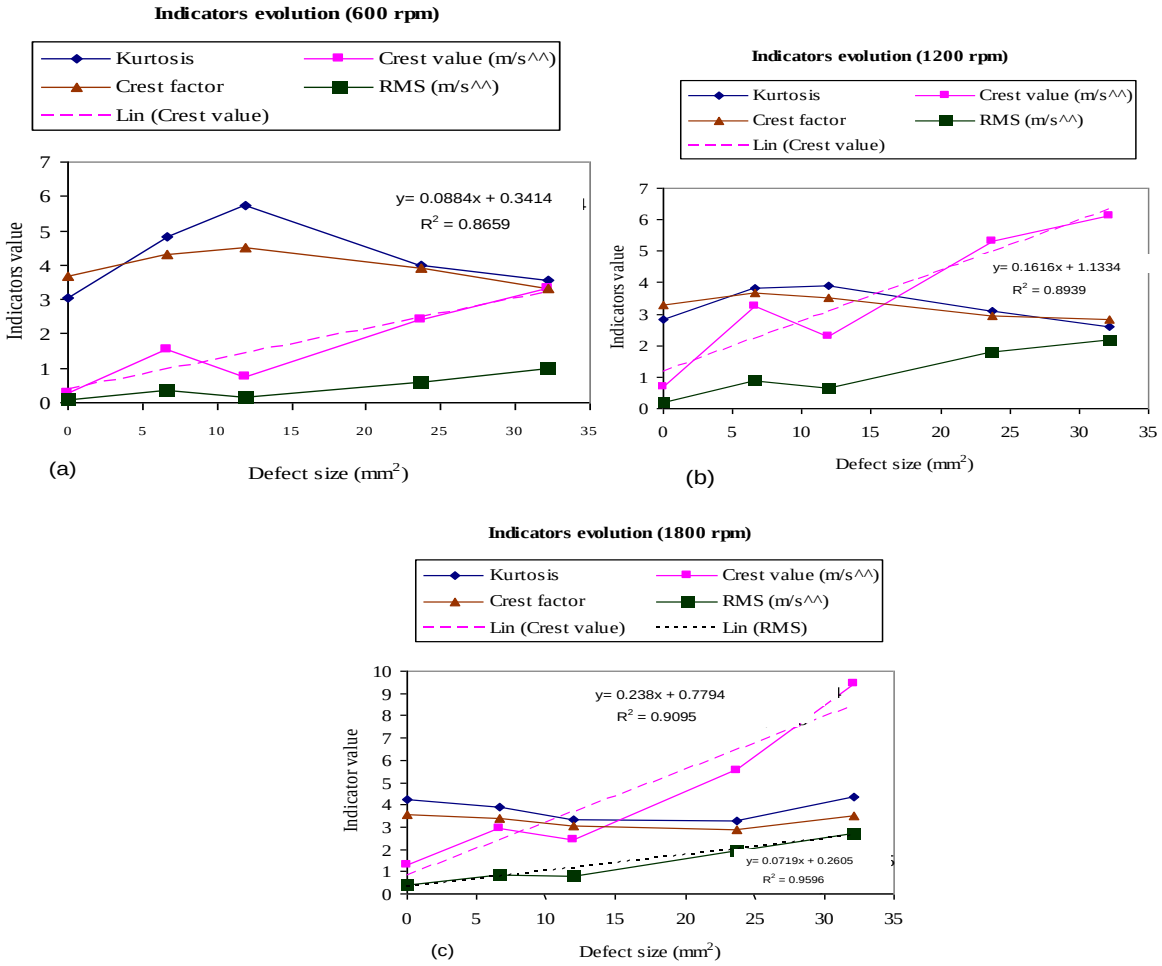

Figure 7. Evolution curve indicators at operating conditions: load 3000 daN. (a) speed 600 rpm; (b) speed 1200 rpm; (c) speed 1800 rpm.

to monitor the defect evolution with different rotation speeds and through several different vibratory indicators (Hoeprich, 1992) known as:

(i) The kurtosis: Is a statistical parameter to analyze the distribution of vibration amplitudes contained in a time signal. It corresponds to the moment of order four and has been shown that for a Gaussian distribution; its value is 3 ± 8%.

$$Kurtosis = \frac{M_4}{M_2^2} = \frac{\frac{1}{N}\sum_{n=1}(x(n)-\bar{x})^4}{\left[\frac{1}{N}(x(n)-\bar{x})^2\right]^2} \quad (4)$$

where x(n) represents the amplitude of the signal for the sample, $\bar{x}$ the average amplitude, σ² variance (moment of order 2) and N the number of samples in the signal.

(ii) The crest value: is the maximum absolute value reached by the representative function of the signal during the time period.

(iii) The crest factor: Is the ratio of the crest value and the signal of root mean square (RMS) value (effective value).

$$Crest\ factor = \frac{Crest\ value}{RMS\ value} = \frac{\sup[x(n)]}{\sqrt{\frac{1}{N}\sum_{n=1}^{N}[x(n)]^2}} \quad (5)$$

where N is number of samples taken from the signal × (n) the discrete time signal.

(iv) The RMS: The expression of the effective value is given by the following equation.

$$V_{effective} = V_{RMS} = \sqrt{\frac{1}{N}\sum_{n=1}^{N}[x(n)]^2} \quad (6)$$

The evolution curves of the statistical indicators obtained at different speeds are shown in Figure 7. According to the indicator evolution curves obtained, we note that the crest value and RMS

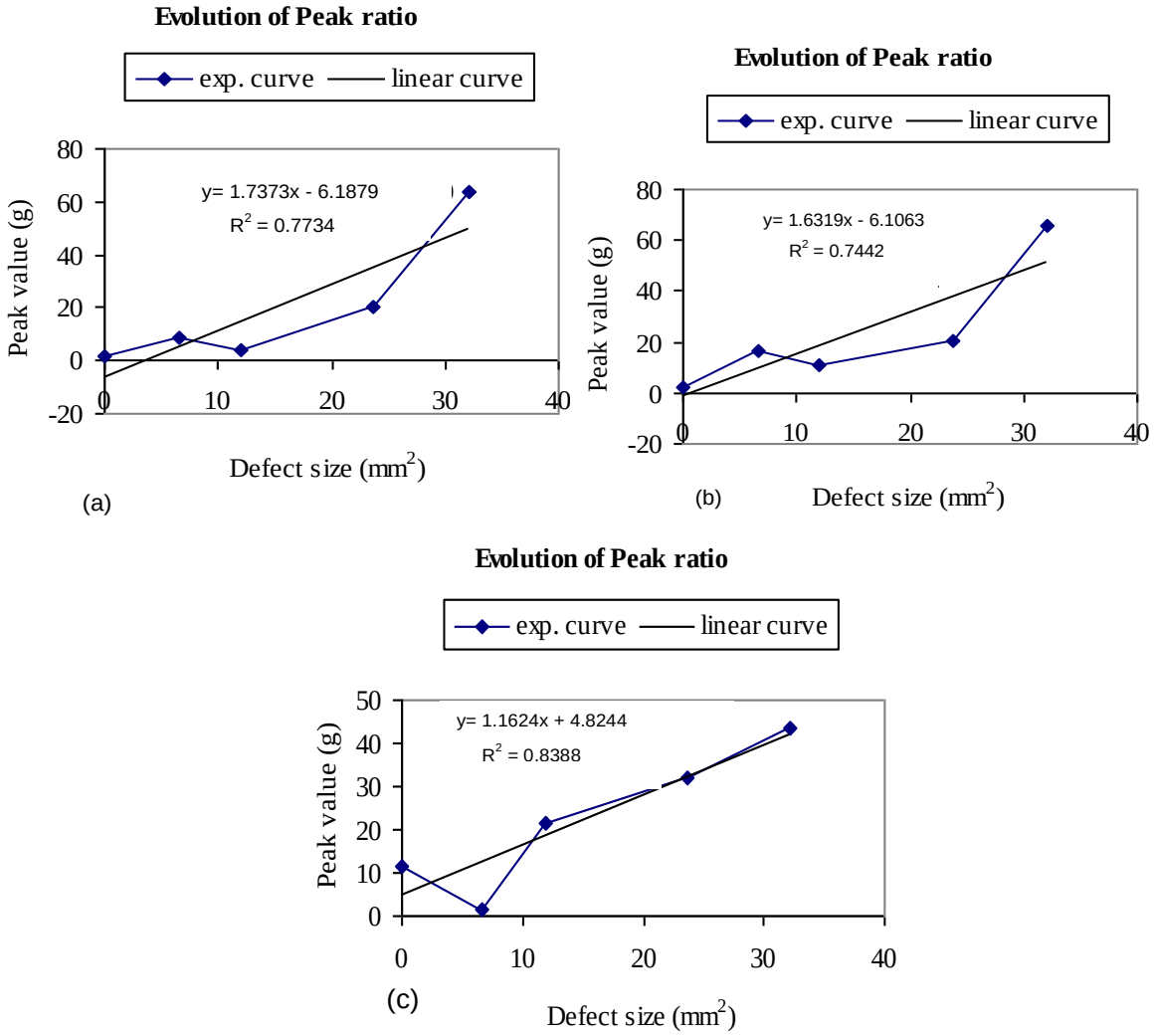

Figure 8. Evolution curve indicator at operating conditions load 3000 daN: (a) speed 600 rpm, (b) speed 1200 rpm, (c) speed 1800 rpm.

indicators are more significant in terms of sensitivity and linearity (see the director coefficient and the correlation coefficient of the linear equation).

(2) Using peak ratio indicator: We use another indicator to monitor the spalling bearing called peak ratio (peak value) (Shiroishi et al., 1997, 1999) of determining the first harmonic amplitude value of the defect frequency for each signal. When it verifies that a defect is present, the peak value is then used to estimate the size (magnitude) of the defect. To calculate the characteristic frequency of the thrust bearing defect, using the following formula (Harris, 1991).

$$F_d = \frac{N_b}{2}(RPS)\left(1+\frac{d_b}{D_p}\cos\beta\right) \quad (7)$$

N_b: Number of balls, RPS: shaft speed, db: ball diameter, Dp: average diameter of the bearing, β: contact angle, for thrust bearing β=0.

A Matlab algorithm called chibora prepared by the LMA-Grespi laboratory is used to transform the vibration signal collected at the test bench to frequency spectrum. We show the evolution of the defect indicator at different speeds in Figure 8.

DISCUSSION

The diameters of the imprints examined, ranged from 2.9 to 6.4 mm and composed of the remarkable defects on the thrust bearing. This was found through the evolution curves of vibratory indicators such as crest value, RMS and peak value. We have proposed an approach based on two criteria to choose the optimum indicator: The

sensitivity and linearity. The indicators sensitive to the default progression are the crest value, the peak value and the RMS that we can justify through linear equations as they were given in Figures 7 and 8 for the rotational speed of 1800 rpm (Li et al., 1999). This case was cited as an example because we find that sensitivity increases with the rotational speed. Otherwise, the RMS indicator moves with more linearity according the defect size by the correlation coefficient (R^2=0.956) in Figure 7c for the same rotational speed. Similarly, the linearity increase with the rotational speed as it is shown in Figure 7 for the crest value.

Conclusion

To make a judicious choice of the vibratory indicator, we must establish a compromise between sensitivity and linearity. Consequently, the evolution of the peak ratio (peak value) indicator is more significant in term of sensitivity. Otherwise the evolution of the RMS indicator is more interesting in term of linearity. Therefore, the evolution of the bearing damage could be relatively expressed by the peak ratio (peak value) indicator or crest value indicator.

REFERENCES

Daniel G, Fabrice V, Roger G, Gilles D (2002). Rolling Contact Fatigue Tests to Investigate Surface Initiated Damage Using Surface Dents. Bearing steel technology, ASTM STA. P. 1419.

Harris TA (1991). Rolling Bearing Analysis. John Wiley & Sons, Inc. New York. 3rd Edition.

Hoeprich MR (1992). Rolling Element Bearing Fatigue Damage Propagation. J. Tribol. P. 114.

Li Y, Billington S, Zhang C (1999). Adaptive prognostics for rolling element bearing condition. Mech. Syst. Signal Process. 13(1):103-113.

Michael N, Tedric A, Harris (2001). Fatigue Failure Progression in Ball Bearings. Transactions of the ASME. J. Tribol. 123(238).

Michel A, René B (2005). Systèmes Mechanical systems. Theory and Dimensioning, DUNOD. 661, ISBN-102100491040.

Nagi G, Mark L (2004). Residual Life Prediction From Vibration-Based Degradation Signals: A Neural Network Approach. IEEE Trans. Ind. Elect. 51(3).

Robert BR, Jerome A (2011). Rolling element bearing Diagnostics. Mech. Syst. Signal Process. pp. 485-520.

Shiroishi J, Li Y, Liang S, Kurfess T, Danyluk S (1997). Bearing Condition Diagnostics Via Vibration and Acoustic Emission Measurements. Mech. Syst. Signal Process. pp. 693-705.

Shiroishi J, Li Y, Liang S, Kurfess T, Danyluk S (1999). Vibration Analysis for Bearing Outer Race Condition Diagnostics. J. Braz. Soc. Mech. Sci. 21(3):484-492.

Tallian TE (1992). Simplified Contact Fatigue Life Prediction Model – Part 1: Review of Published Models. Trans. ASME. J. Tribol. 114:207-213.

Youngsik C, Richard L (2007). Spall progression live model for rolling contact verified by finish hard machined surfaces. Wear 262:24-35.